# Supporting Information

## An Ion-Conducting SnS-$SnS_2$ Hybrid Coating for Commercial Activated Carbons Enabling Their Use as High Performance Anodes for Sodium-Ion Batteries

Si-Wei Zhang, [a] Wei Lv,[*b] Dong Qiu, [b] Tengfei Cao, [a] Jun Zhang, [a] Qiaowei Lin, [b] Xiangrong Chen, [b] Yanbing He, [b] Feiyu Kang [ab] and Quan-Hong Yang [c]

[a] Tsinghua-Berkeley Shenzhen Institute (TBSI), Tsinghua University, Shenzhen 518055, China

[b] Shenzhen Geim Graphene Center (SGC), Engineering Laboratory for Functionalized Carbon Materials, Graduate School at Shenzhen, Tsinghua University, Shenzhen 518055, China. E-mail: lv.wei@sz.tsinghua.edu.cn

[c] Nanoyang Group, State Key Laboratory of Chemical Engineering, School of Chemical Engineering and Technology, Tianjin University, Tianjin 300072, China. E-mail: qhyangcn@tju.edu.cn

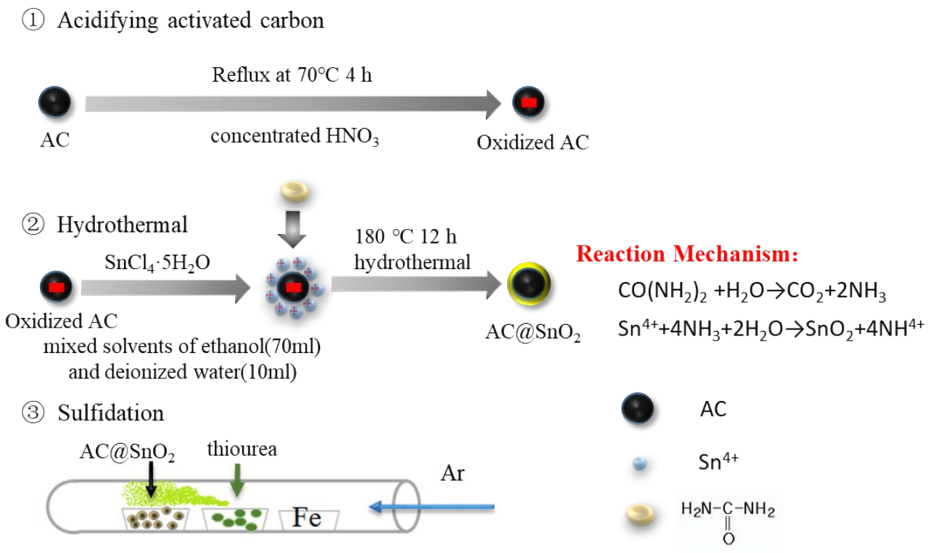


**Scheme S1**. Schematic illustration of the preparation process of the AC@SnS-$SnS_2$.

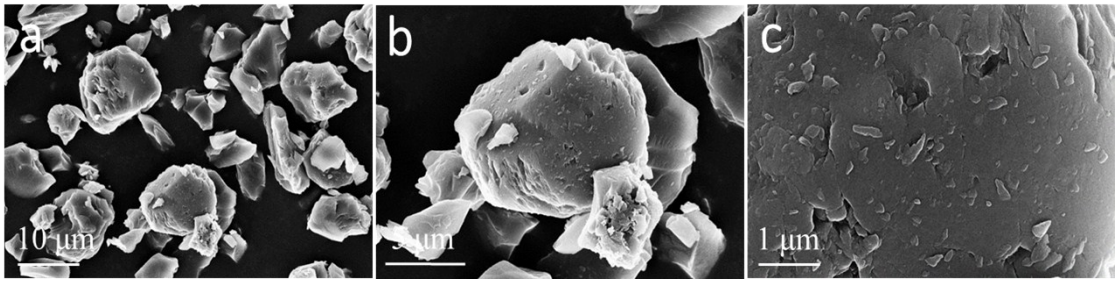


**Figure S1.** SEM images of the oxidized AC.

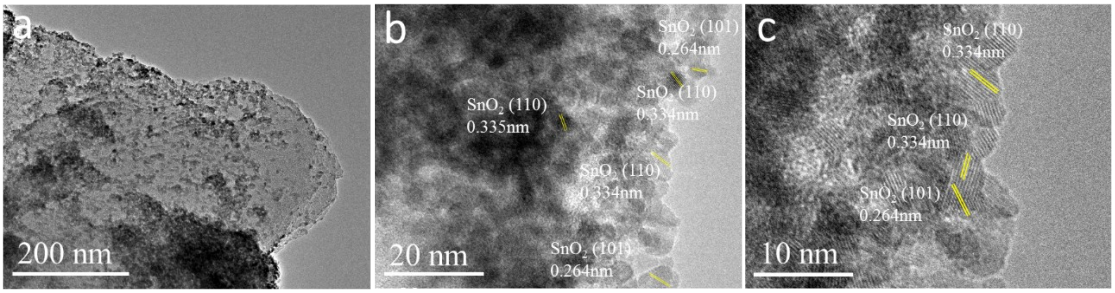


**Figure S2.** (a) TEM image and (b-c) HRTEM images of the AC@$SnO_2$.

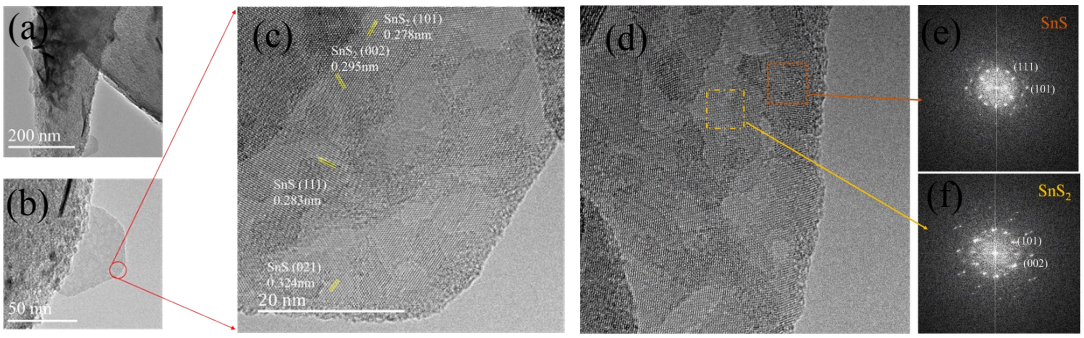


**Figure S3.** TEM images (a-c) and Fast Fourier transform (FFT)-diffraction (d-f) of the SnS-$SnS_2$ hybrid nanosheets on the surface of the AC.

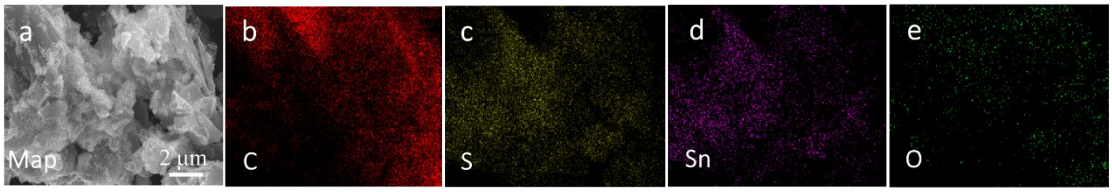


**Figure S4.** (a) SEM image and (b) C, (c) S, (d) Sn, (e) O element mappings of the AC@SnS-$SnS_2$.

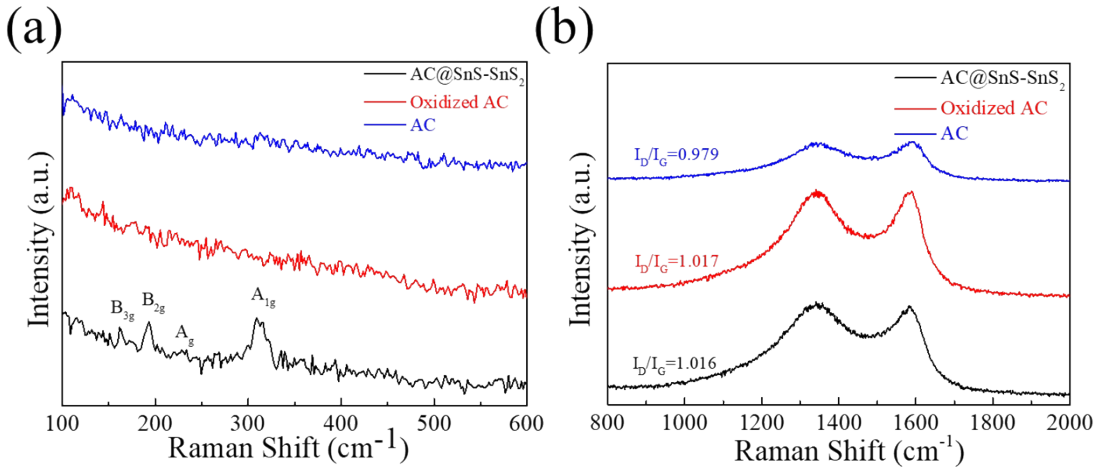


**Figure S5.** Raman spectra of AC, oxidized AC and AC@SnS-$SnS_2$.

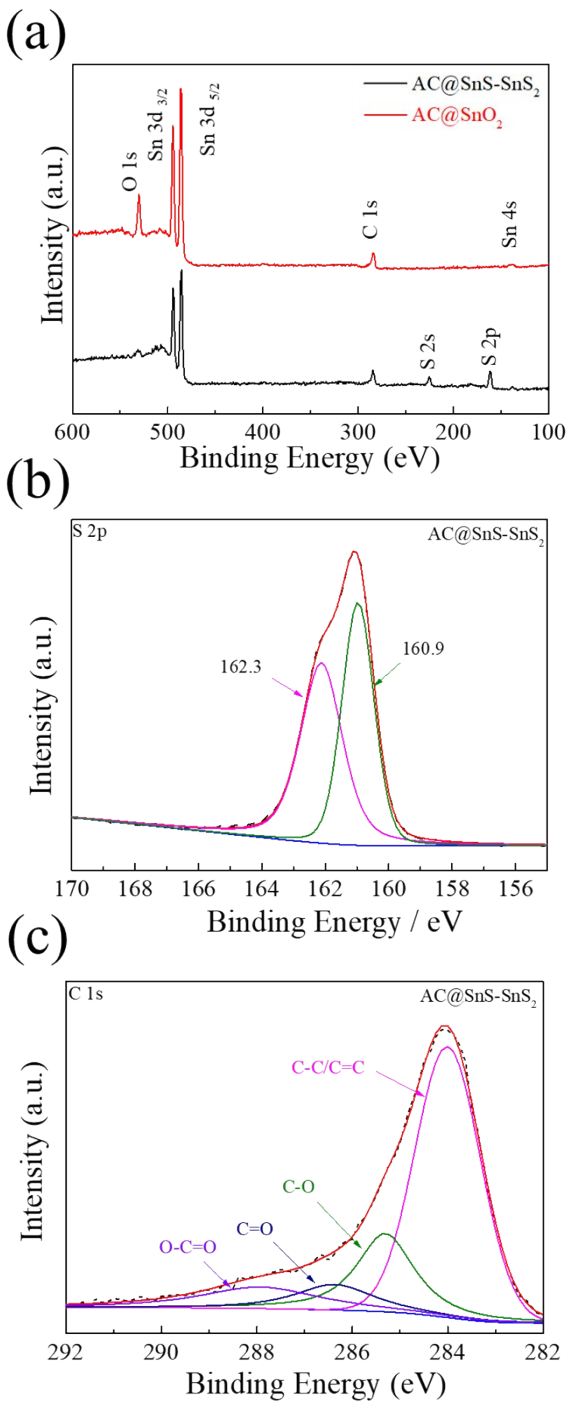


**Figure S6.** (a) Typical XPS survey spectra of AC@SnS-$SnS_2$ and AC@$SnO_2$, (b) S 2p, and (c) C 1s XPS spectra of the AC@SnS-$SnS_2$.

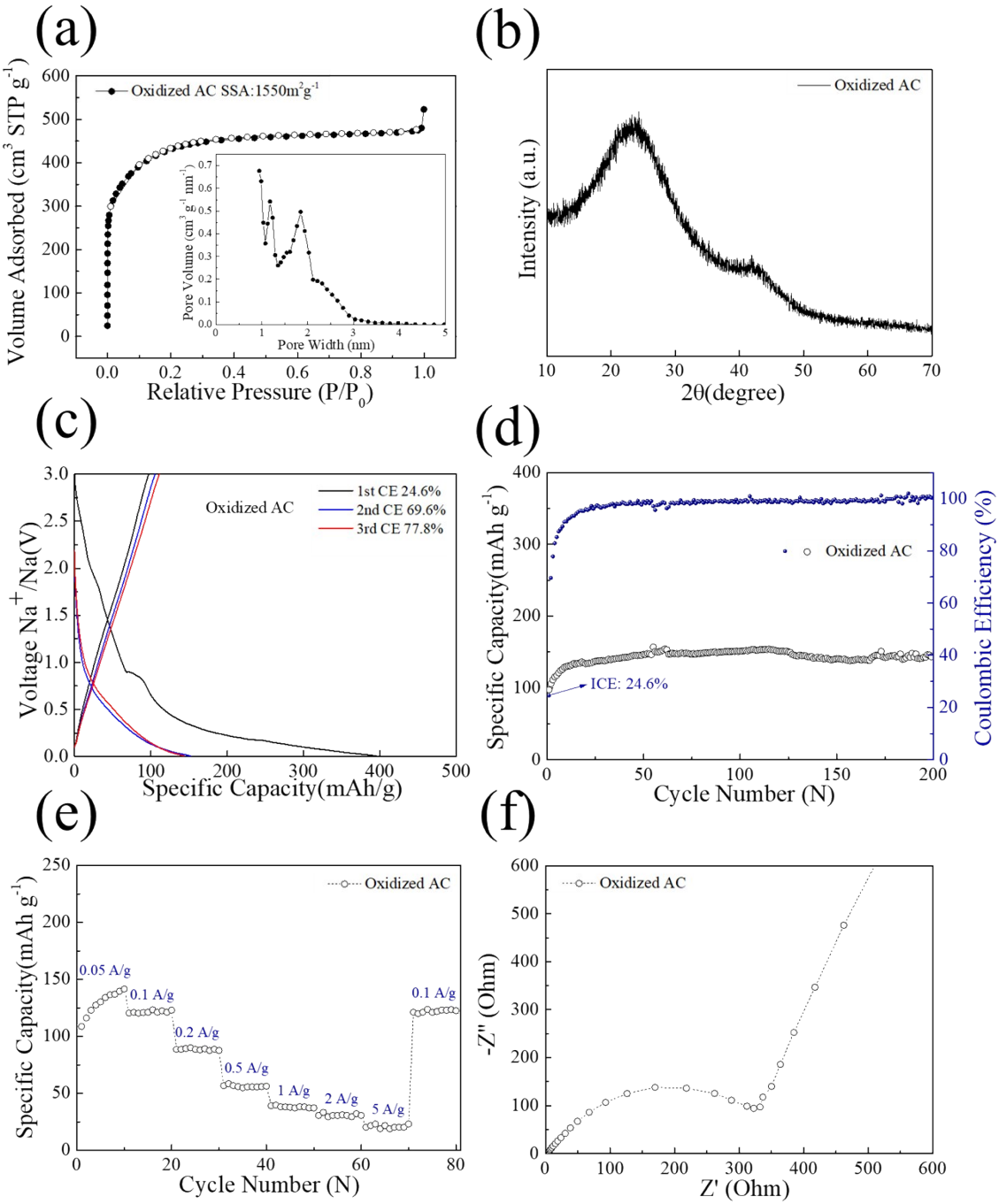


**Figure S7.** Structural and electrochemical characterization of the oxidized AC. (a) Nitrogen adsorption isotherm with the pore size distribution, (b) XRD pattern, (c) galvanostatic charge-discharge profiles, (d) cyclic performance at a current density of 0.1 A $g^{-1}$, (e) rate performance, and (f) Nyquist plots of the oxidized AC.

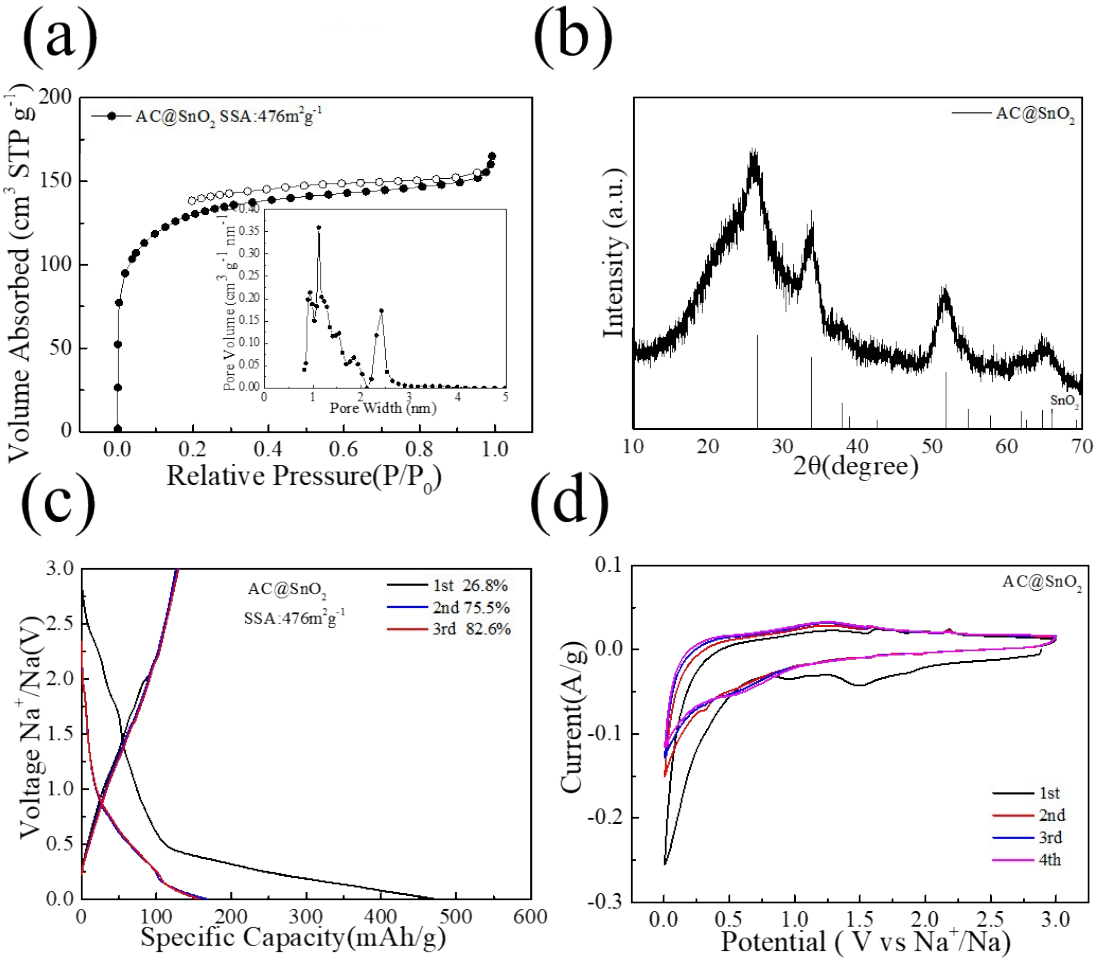


**Figure S8.** Structural and electrochemical characterization of the AC@$SnO_2$. (a) Nitrogen adsorption isotherm with the inserted pore size distribution, (b) XRD pattern, (c) galvanostatic charge-discharge profiles, and (d) Nyquist plots of the AC@$SnO_2$.

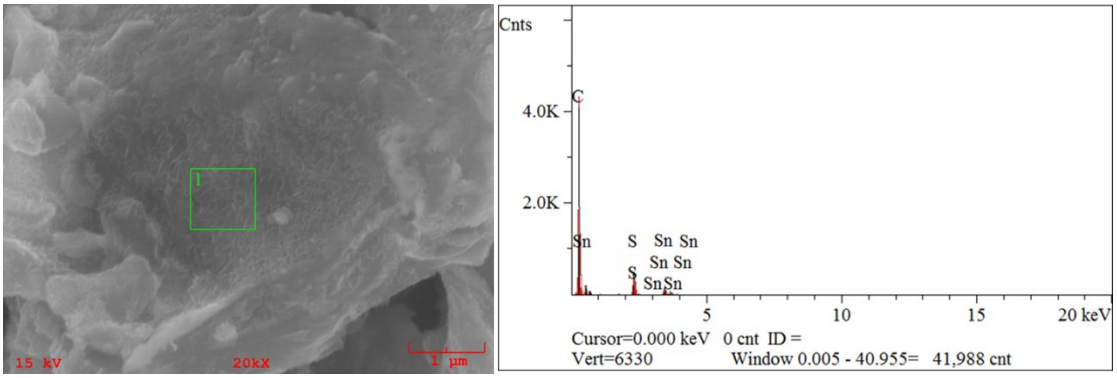


| Element | Intensity (c/s) | Atomic (%) | Mass (%) |
|---|---|---|---|
| C | 360.84 | 80.63 | 61.89 |
| O | 34.76 | 13.46 | 13.76 |
| S | 103.92 | 3.70 | 7.58 |
| Sn | 37.35 | 2.21 | 16.77 |

**Figure S9.** EDS spectrum of the AC@SnS-$SnS_2$. Wide area EDS analysis indicated the existing of 2.21% Sn and 3.697% S (atomic ratio), so the corresponding ratio of $SnS_2$ is 1.497% and SnS is 0.703%, and the $Sn^{4+}/Sn^{2+}$ mole ratio is about 2.13, suggesting the formation of the SnS-$SnS_2$ hybrids. (The $Sn^{4+}/Sn^{2+}$ ratio measured with XPS is estimated to be around 2.15).

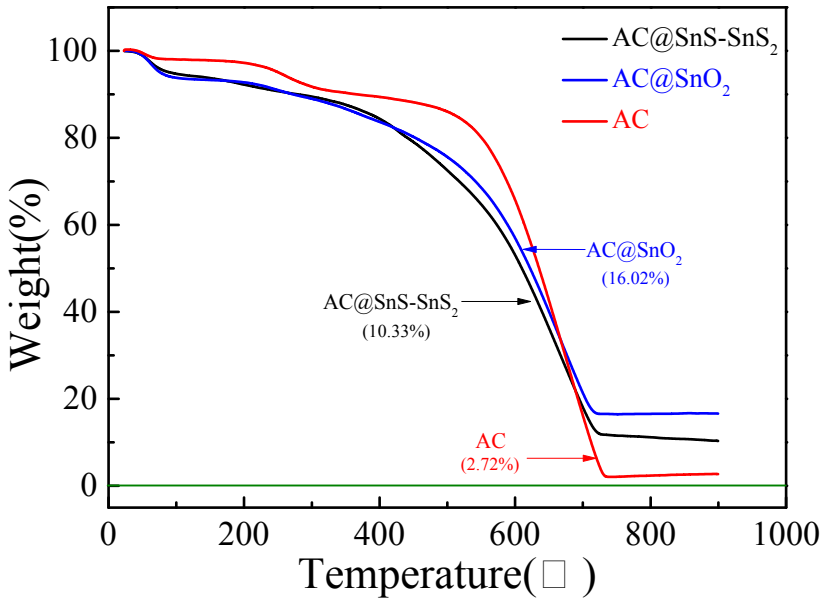


**Figure S10.** TGA curves of AC@SnS-$SnS_2$, AC@$SnO_2$, and AC. The AC has 2.72 wt% impurities which can't be burned before treated by $HNO_3$. Since the $Sn^{4+}/Sn^{2+}$ ratio is about 2.1, the amounts of $SnS_2$ and SnS in the AC@SnS-$SnS_2$ are about 8.47 wt% and 3.34 wt%.

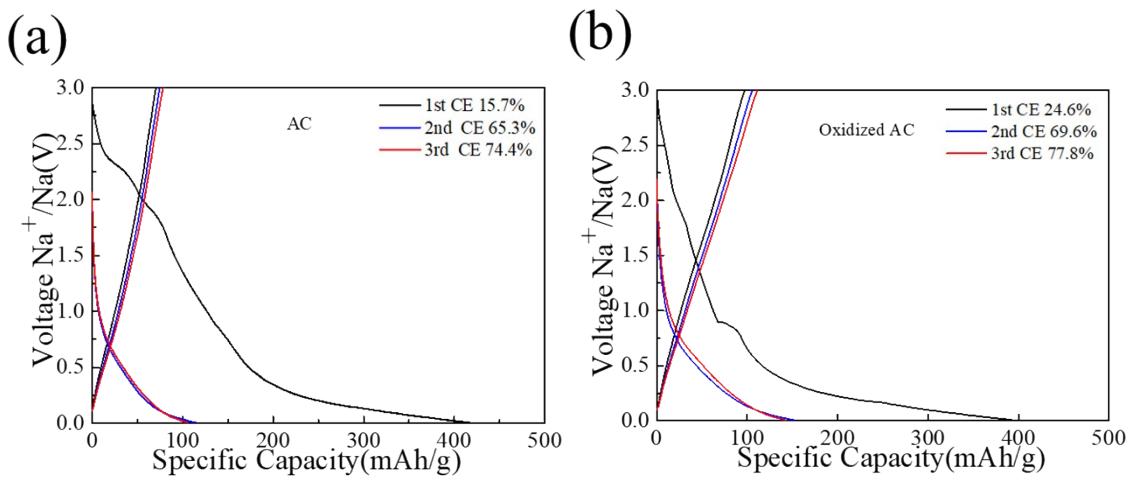


**Figure S11.** Galvanostatic charge-discharge curves of (a) AC and (b) oxidized AC at a current density of 0.1 A $g^{-1}$.

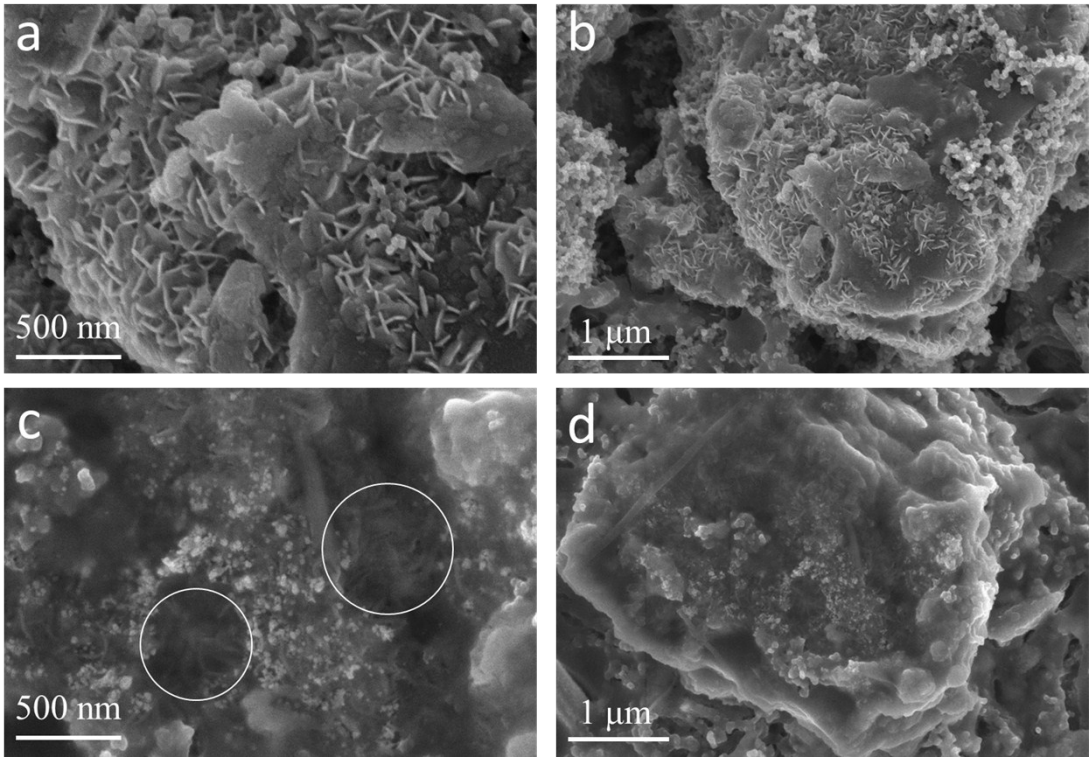


**Figure S12**. The SEM images of the AC@SnS-$SnS_2$ electrode (a and b) before and (c and d) after 100 cycles charge/discharge at a current density of 0.3 A $g^{-1}$.

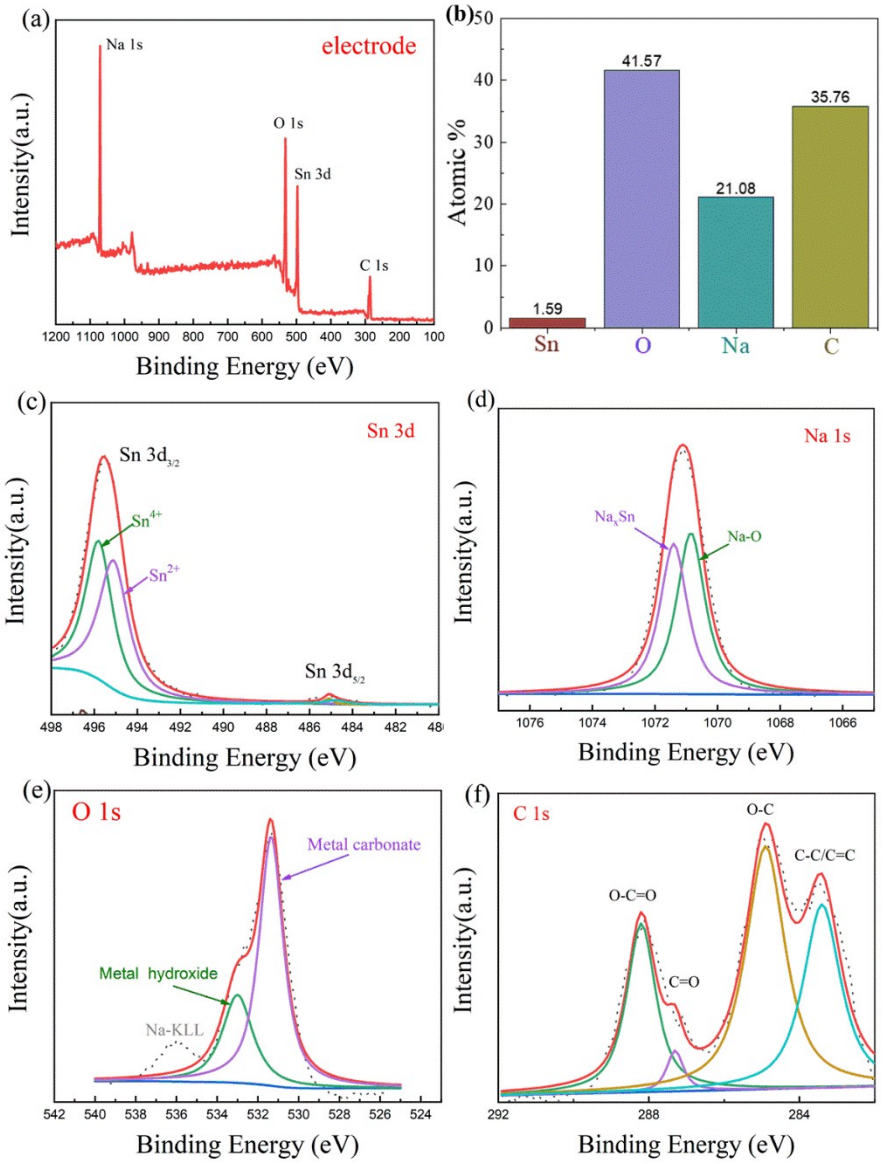


**Figure S13.** XPS results of cycled AC@SnS-$SnS_2$ electrode. (a) XPS survey spectra; (b) atomic contents; (c) Sn 3d; (d) Na 1s; (e) O 1s and (f) C 1s profiles

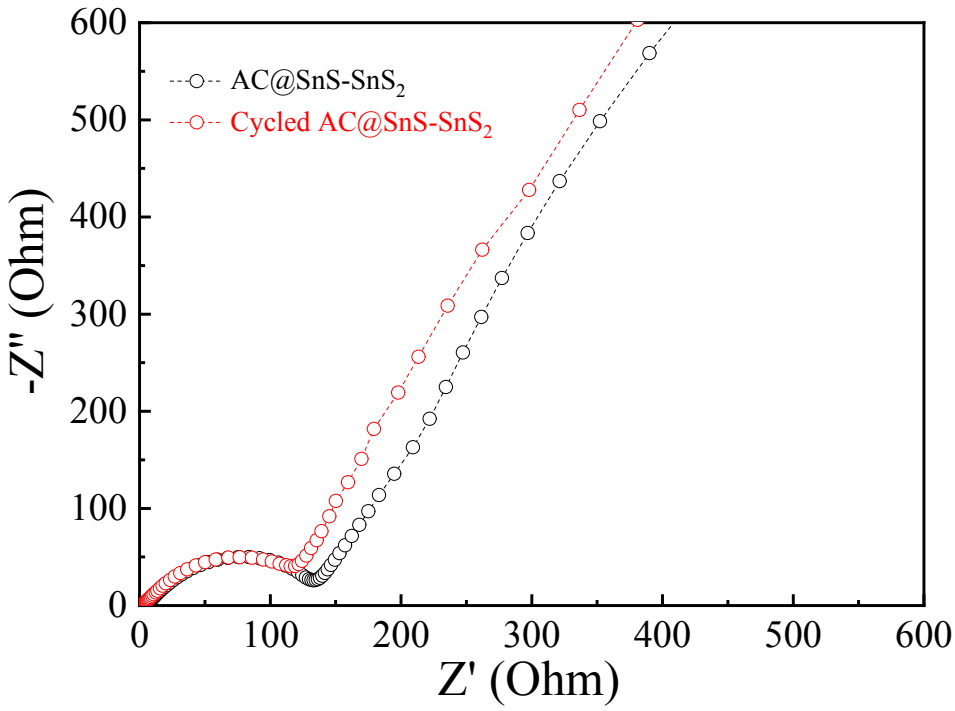


**Figure S14.** Nyquist plots of AC@SnS-$SnS_2$ before and after 10 cycles

**Table S1.** The comparison of the sodium storage performance of the AC@SnS-$SnS_2$ vs. other coatings on porous carbon materials.

| Materials | ICE (%) | Rate performance | Reference |
|---|---|---|---|
| CNTs/CFP@$TiO_2$ | 43.6 | 128.6 mA h $g^{-1}$ at 2 A $g^{-1}$ | [1] |
| HPC@G | / | 250 mA h $g^{-1}$ at 1 A $g^{-1}$ | [2] |
| CNT@$SnO_2$ @G | 43 | 97 mA h $g^{-1}$ at 1 A $g^{-1}$ | [3] |
| Porous carbon/$TiO_2$ | / | 120 mA h $g^{-1}$ at 0.11 A $g^{-1}$ | [4] |
| NC/$TiO_2$ | 37.3 | 104 mA h $g^{-1}$ at 3.3 A $g^{-1}$ | [5] |
| SnS@rGO | 42 | 240 mA h $g^{-1}$ at 0.4 A $g^{-1}$ | [6] |
| SnS-C | ~60 | 450 mA h $g^{-1}$ at 0.80 A $g^{-1}$ | [7] |
| $SnS_2$/C | ~75 | 80 mA h $g^{-1}$ at 2 A $g^{-1}$ | [8] |
| $SnS_2$/rGO | ~55 | 530 mA h $g^{-1}$ at 2 A $g^{-1}$ | [9] |
| $SnS_2$/graphene | ~50 | 337 mA h $g^{-1}$ at 12.8 A $g^{-1}$ | [10] |
| AC@SnS-$SnS_2$ | 68.6 | 110 mA h $g^{-1}$ at 5 A $g^{-1}$ | This Work |

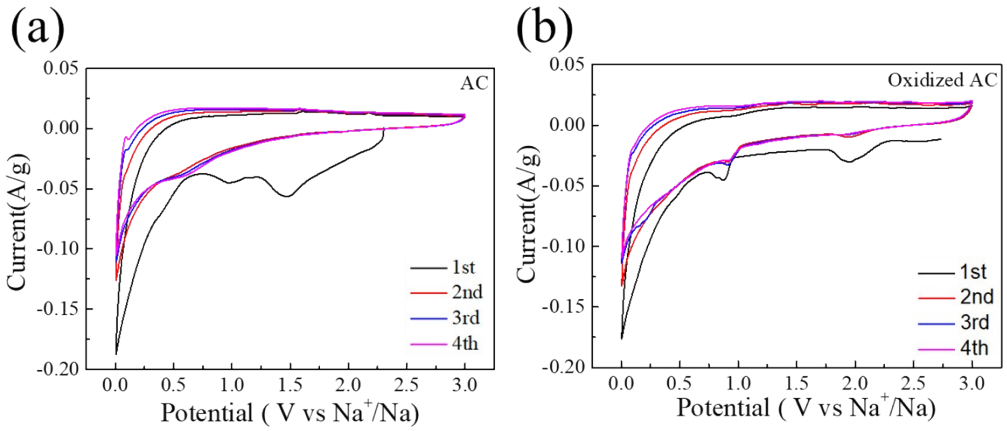


**Figure S15.** CV curves of (a) AC and (b) oxidized AC at a scan rate of 0.1 mV $s^{-1}$.

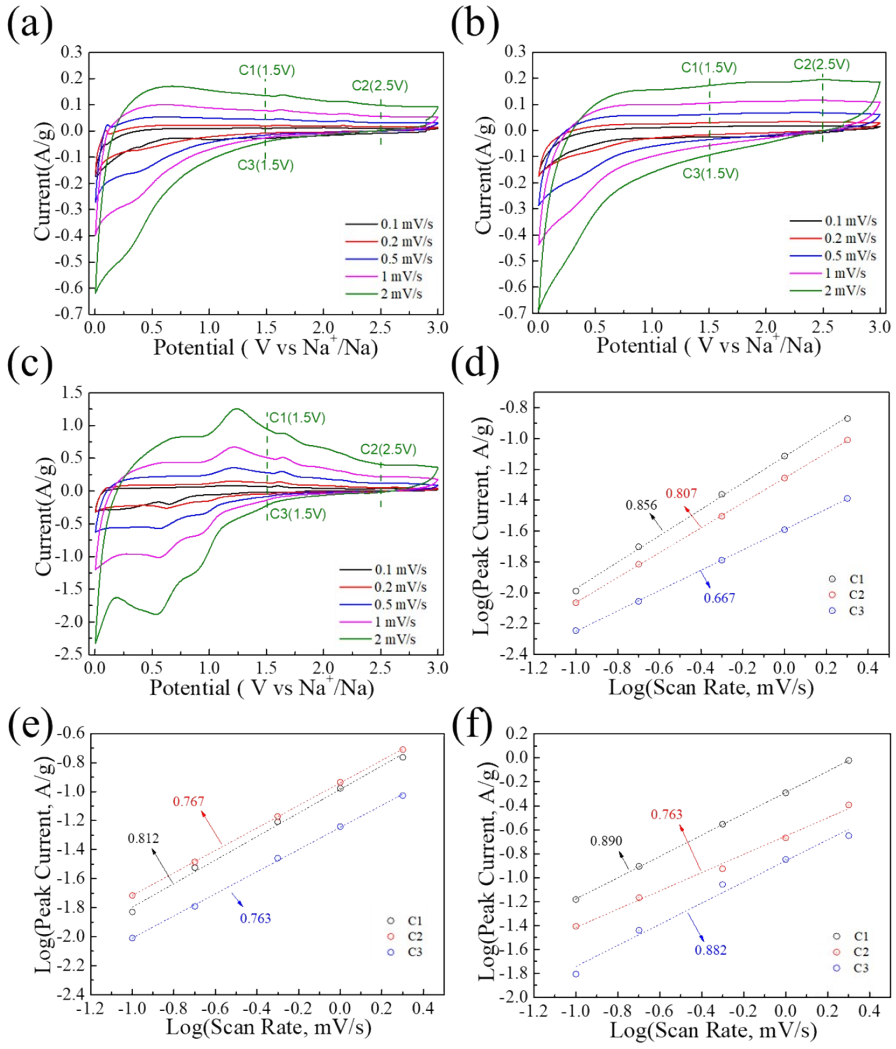


**Figure S16.** CV curves at various scan rates from 0.1 mV $s^{-1}$ to 2 mV $s^{-1}$ of the (a) AC, (b) oxidized AC and (c) AC@SnS-$SnS_2$; Determination of the *b* values for various selected conditions for (d) AC, (e) oxidized AC and (f) AC@SnS-$SnS_2$.

**Table S2.** Parameters of equivalent circuit modeling of EIS spectra of different samples.

| Samples | $R_s/\Omega$ | $R_{ct}/\Omega$ | $D/cm^{-2}s^{-1}$ |
|---|---|---|---|
| AC@SnS-SnS2 | 4.7 | 136.1 | $7.67\times10^{-13}$ |
| AC@SnO2 | 5.2 | 323.6 | $6.58\times10^{-13}$ |
| AC | 4.9 | 342.5 | $4.39\times10^{-13}$ |

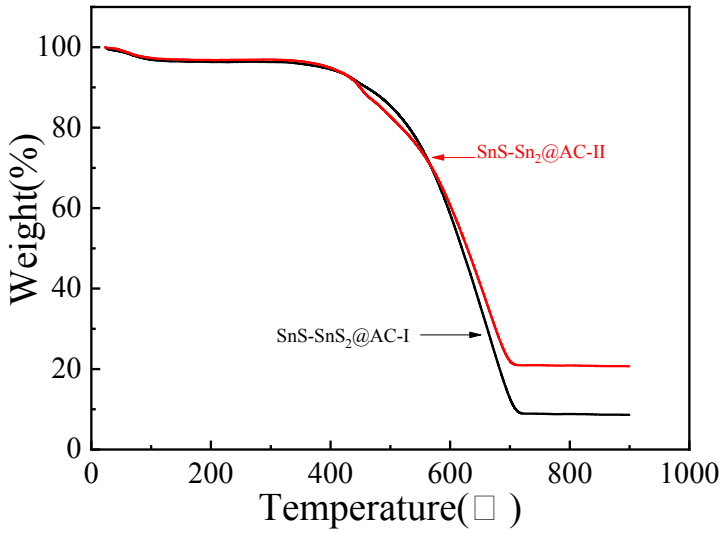


**Figure S17.** TGA curves of AC@SnS-$SnS_2$- Ⅰ and AC@SnS-$SnS_2$- Ⅱ

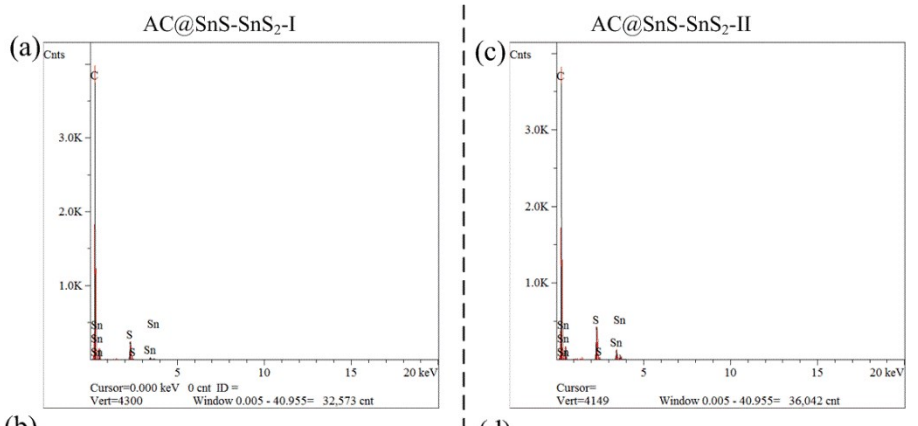


(b)

| Elt. | Atomic (%) | Mass (wt.%) |
|---|---|---|
| C | 84.06 | 74.02 |
| O | 14.03 | 16.46 |
| S | 1.12 | 2.74 |
| Sn | 0.79 | 6.78 |

(d)

| Elt. | Atomic (%) | Mass (wt.%) |
|---|---|---|
| C | 80.75 | 62.36 |
| O | 13.51 | 13.86 |
| S | 3.57 | 7.48 |
| Sn | 2.17 | 16.30 |

**Figure S18.** EDS results of the AC@SnS-$SnS_2$- Ⅰ and AC@SnS-$SnS_2$- Ⅱ

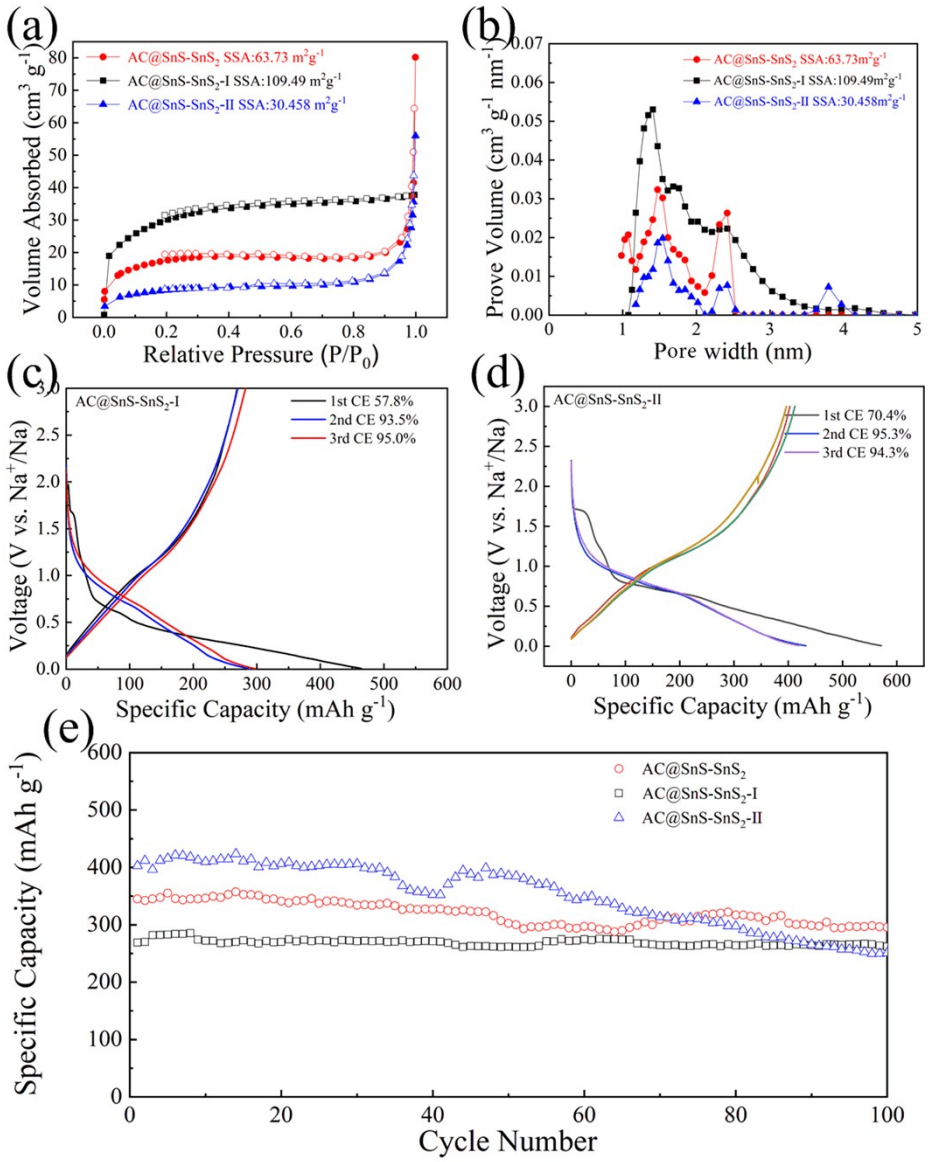


**Figure S19.** Structure and electrochemical characterization of the AC with different contents of SnS-$SnS_2$ hybrid. (a) Nitrogen adsorption isotherms; (b) Pore size distributions; and Galvanostatic charge-discharge profiles of AC@SnS-$SnS_2$-Ⅰ (c) and AC@SnS-$SnS_2$-Ⅱ (d) at a current density of 0.1 A $g^{-1}$; (e) Cycling performance of them at 0.1 A $g^{-1}$.

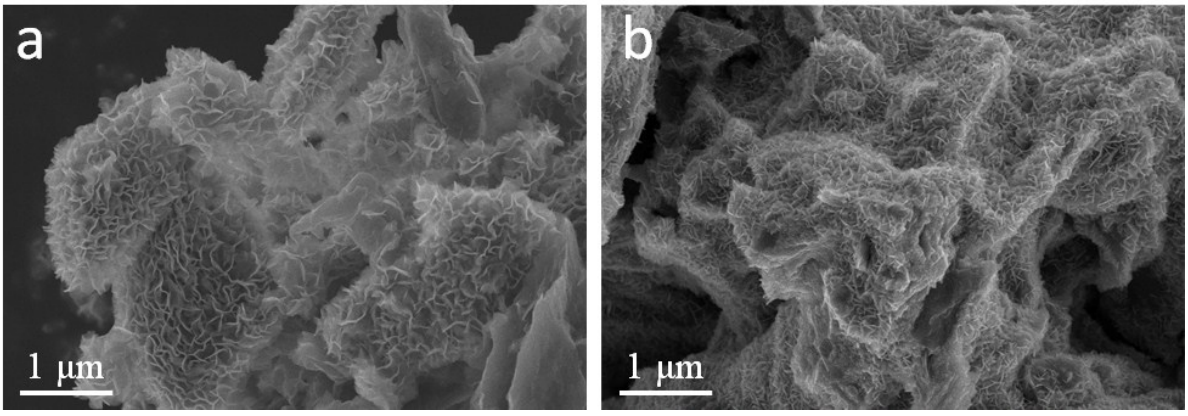


**Figure S20**. SEM images of (a) AC@$SnS_2$ and (b) AC@SnS

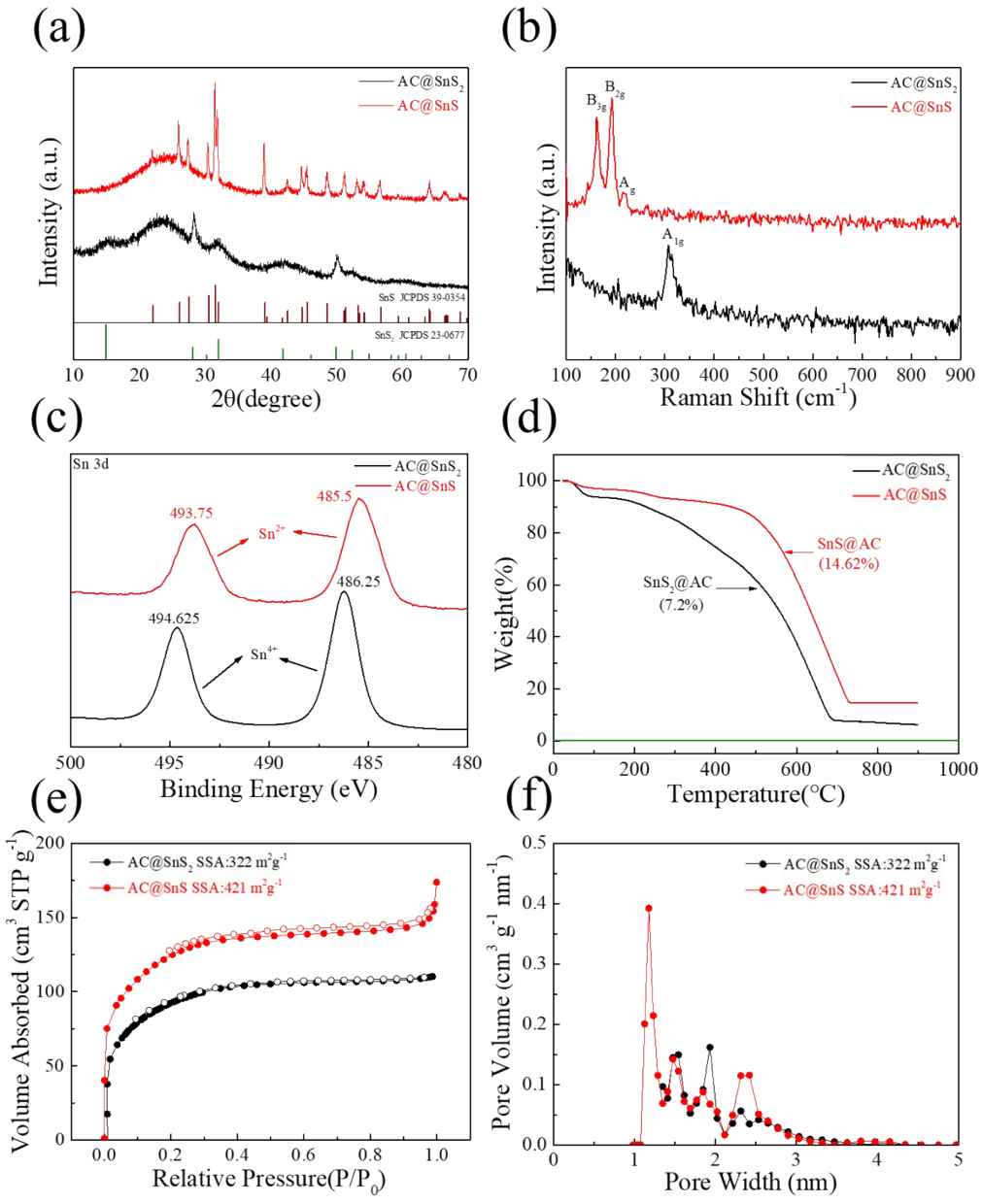


**Figure S21.** (a) XRD patterns, (b) Raman spectra, (c) Sn 3d XPS spectra, (d) TGA curves, (e) $N_2$ adsorption isotherms, and (f) pore size distributions of AC@$SnS_2$ and AC@SnS.

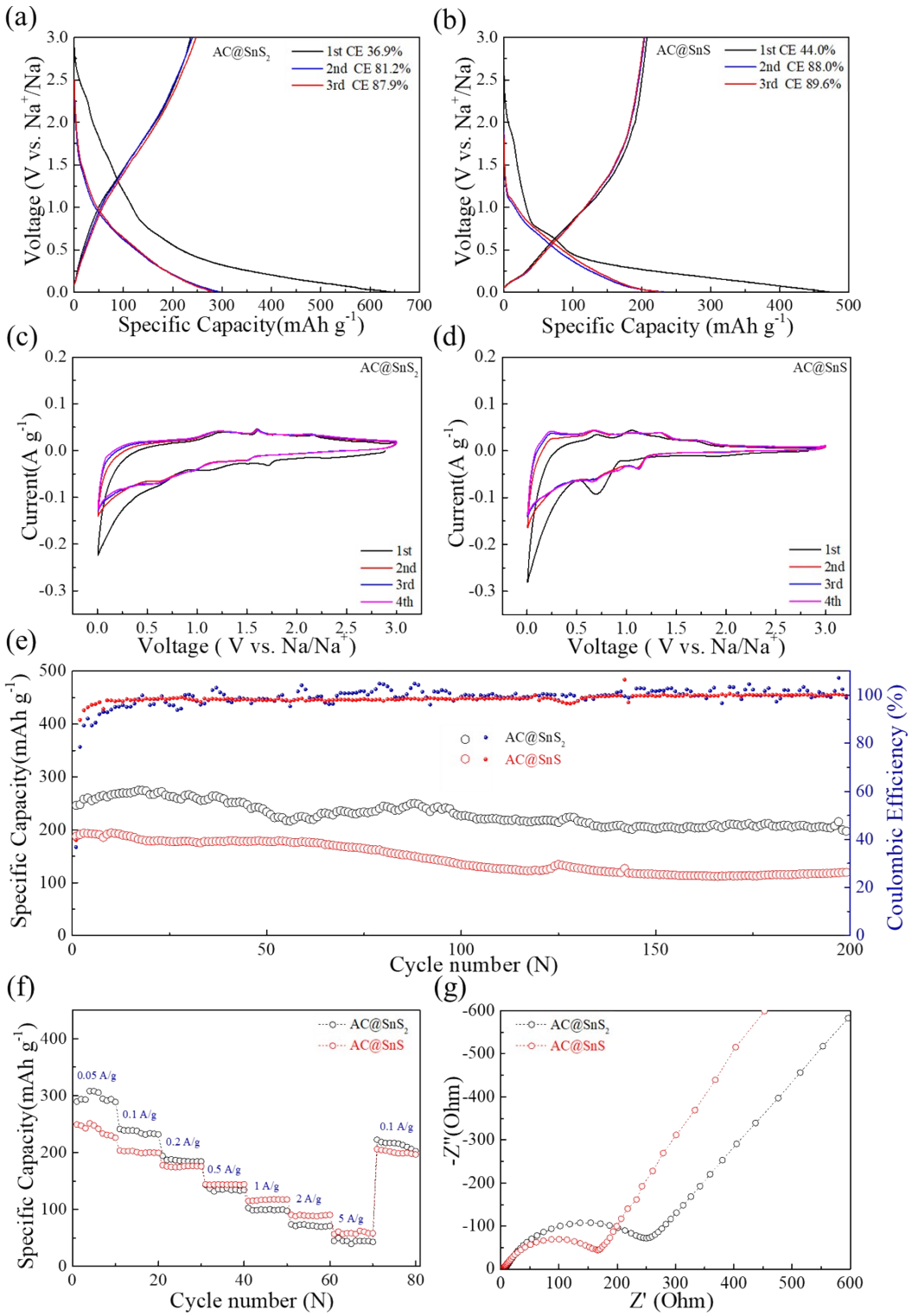


**Figure S22.** (a and b) Galvanostatic charge-discharge profiles for selected cycles of AC@$SnS_2$ and AC@SnS at a current density of 0.1 A $g^{-1}$; (c and d) CV curves of the first four cycles of AC@$SnS_2$ and AC@SnS at a scan rate of 0.1 mV $s^{-1}$; (e) Cyclic performance of AC@$SnS_2$ and AC@SnS at a current density of 0.1 A $g^{-1}$; (f) Rate performance of AC@$SnS_2$ and AC@SnS at current densities ranging from 0.05 A $g^{-1}$ to 5 A $g^{-1}$; (g) Nyquist plots of AC@$SnS_2$ and AC@SnS after the first cycle.

**Results for the other two kinds of AC:**

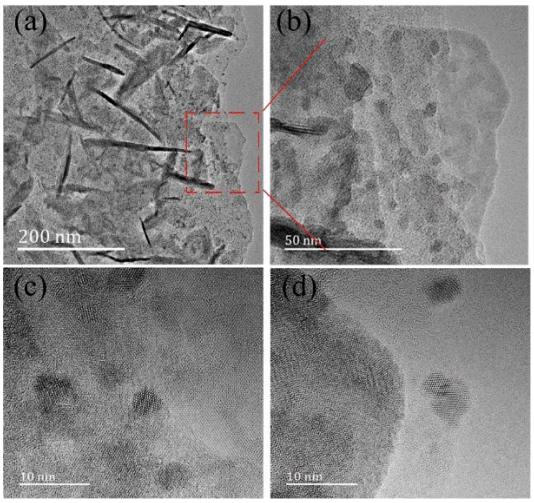


**Figure S23.** TEM images of the AC-2@SnS-$SnS_2$

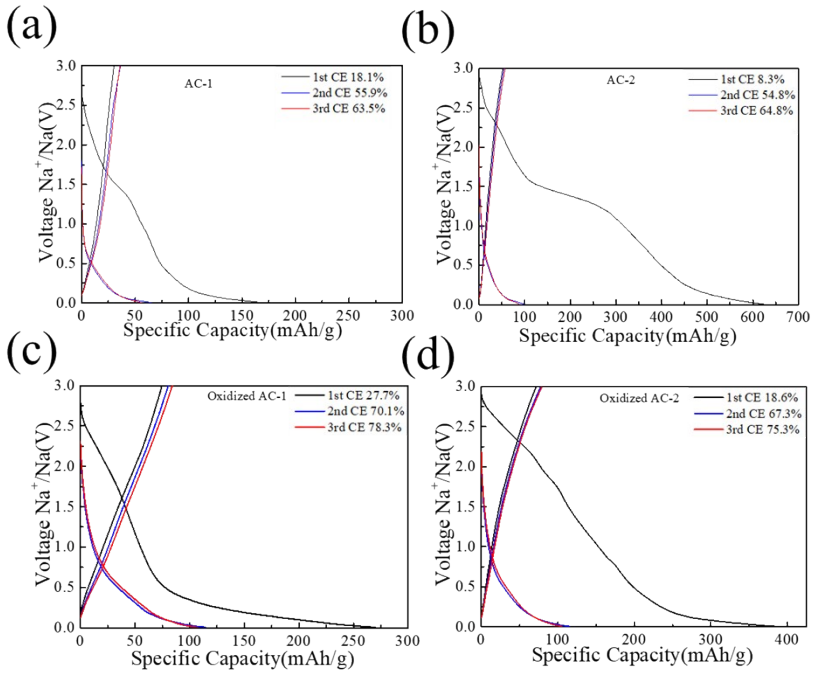


**Figure S24.** Galvanostatic charge-discharge curves of (a and b) the other two kinds of AC, (c and d) the correlated oxidized ACs at a current density of 0.1 A $g^{-1}$.

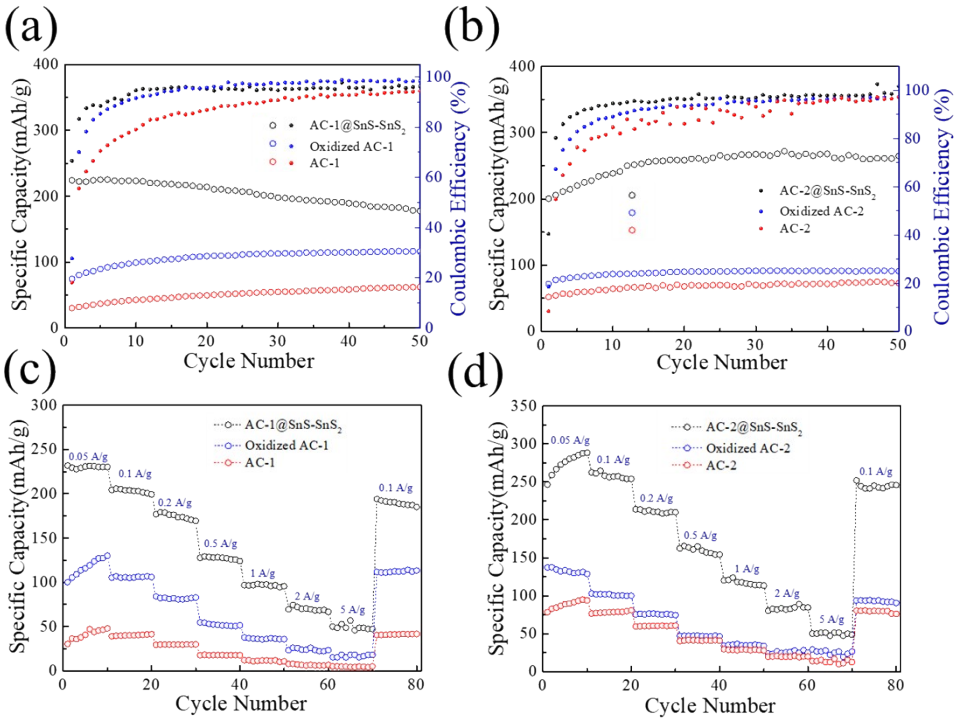


**Figure S25.** (a and b) Cyclic performances at 0.1 A $g^{-1}$ and (c and d) rate performances of the other two kinds of AC, the correlated oxidized ACs and the correlated AC@SnS-$SnS_2$s.

## Reference


[1] H. Wang, G. Jia, Y. Guo, Y. Zhang, H. Geng, J. Xu, W. Mai, Q. Yan, H. J. Fan, *Adv. Mater. Interfaces*, **2016**, 3, 1600375.

[2] Y. Yan, Y.-X. Yin, Y.-G. Guo, L.-J. Wan, *Adv. Energy Mater.*, **2014**, 4, 1301584.

[3] D. Zhou, X. Li, L.-Z. Fan, Y. Deng, *Electrochimica Acta*, **2017**, 230, 212–221.

[4] J. Lee, Y.-M. Chen, Y. Zhu, B. D. Vogt, *ACS Appl. Mater. Interfaces,* **2014**, 6, 21011−21018.

[5] X. Zhao, C. Yan, X. Gu, L. Li, P. Dai, D. Li, H. Zhang, *ChemElectroChem*, **2017**, 4, 1516–1522.

[6] L. Wu, H. Lu, L. Xiao, X. Ai, H. Yang, Y. Cao, *J. Power Sources* **2015**, *293*, 784–789.

[7] L. Wu, H. Lu, L. Xiao, J. Qian, X. Ai, H. Yang, Y. Cao, *J. Mater. Chem. A* **2014**, *2*, 16424–16428.

[8] B. Qu, C. Ma, G. Ji, C. Xu, J. Xu, Y. Meng, T. Wang, J. Lee, *Adv. Mater.* **2014**, *26*, 3854–3859.

[9] X. Xie, D. Su, S. Chen, J. Zhang, S. Dou, G. Wang, *Chem. Asian J.* **2014**, *9*, 1611–1617.

[10] Y. Zhang, P. Zhu, L. Huang, J. Xie, S. Zhang, G. Cao, X. Zhao, *Adv. Funct. Mater.* **2015**, *25*,481–489.